Surface Forces and Fracture in Brittle Materials†

*B. R. Lawn and S. Lathabai**

SYNOPSIS. The role of surface forces in the fracture of intrinsically brittle materials (ceramics) in chemical environments is examined. It is asserted that fundamental intersurface potential functions of the type directly measurable in the 'crossed cylinder' surface force apparatus of Israelachvili uniquely predetermine the crack mechanics, including healing and regrowth behaviour. The link is formalized by first stating the Griffith-Irwin theorem for equilibrium cracks, and then introducing the intersurface potential via the familiar surface energy term. The surface energy is modified by the adsorption of environmental species between the crack walls. A critical element in our thesis is the presence of atomic-scale oscillations in the surface force function at small separations, corresponding to a short-range ordering influence of the confining solid structure on the intervening molecular species. It is contended that these oscillations should be manifest as metastable equilibrium states in fracture systems. Experimental data from cyclic crack growth tests on mica in moist atmospheres are used to support this contention. The data exhibit a certain hysteresis, in that the load to *repropagate* the cracks through a healed interface is lower than that initially required to *propagate* the cracks through the virgin material. For non-equilibrium configurations the data show strong kinetic characteristics, as represented in familiar crack velocity diagrams. A consideration of the near-tip crack profile indicates that these kinetics are controlled by activated motion (forward *and* backward) of the intrusive molecular species between interstitial sites at a severely constricted interface. Some radical implications of the surface force modelling are discussed: that the driving force arising from environmental interactions may be described in terms of a 'molecular wedge'; that crack velocity thresholds should be seen as a natural manifestation of equilibrium states (including metastable states) in the underlying force–separation function; and that crack kinetics in most ceramic materials may be controlled by interfacial diffusion processes.

1 INTRODUCTION

It is now known that 'surface forces' govern the laws of brittle fracture [1]. Crack growth is a surface creation process: it follows that the intrinsic cohesive forces which bind surfaces together must control the micromechanics of crack wall separation. This notion is, of course, implicit in the original Griffith concept of fracture [2, 3]. However, it is only recently that the intimate relation between the energetics of fracture and fundamental interatomic potential functions has become fully appreciated. Nowhere is this link more critical than in the description of chemically assisted fracture. In highly brittle materials, notably ceramics, the work to fracture can be drastically reduced by admitting environmental species, especially water, to the crack system, often with strong kinetic effects.

The connection between fracture and surface forces has been given special impetus by the dramatic experiments carried out on mica–mica interactions in various liquid environments by Israelachvili and coworkers at the Australian National University over the past decade [4]. These workers have made *direct measurements* of the potential functions for two surfaces in near-contact. Their apparatus uses mica sheets in crossed-cylinder configuration and monitors the interaction forces down to atomic-level separations. Quite apart from confirming existing theories of *long-range* forces in aqueous solutions (in particular the 'DLVO' theory based on van der Waals attractions and double-layer repulsions), their research has revealed a variety of new *short-range* forces, notably oscillatory 'structural' forces which reflect the ordering influence of the solid structure on intrusive species at molecular-scale separations [5]. Since the cohesive zones for crack tips in ceramic materials are characterized by crack-opening displacements on the same molecular scale, the relevance to brittle fracture becomes clear. For the first time, the opportunity exists for gaining an *independent* measure of the forces that determine the crack energetics in reactive environments.

In this paper we shall attempt to tie the thread between fracture mechanics and surface forces. We begin with a formal statement of Griffith-Irwin fracture mechanics for equilibrium cracks, with the intrinsic surface energy as the characteristic generalized resistive force. We pay particular attention to the way this surface energy may be written for systems influenced by chemical interactions. The surface energy terms are expressed as integrals of interplanar force

† Manuscript received 9 September 1987
* Ceramics Division, National Bureau of Standards, Gaithersburg, MD 20899.

functions over wall–wall separations. It is then shown, with particular reference to the lattice structure of mica, that these force functions must have an oscillatory component of the kind alluded to above, to allow for the geometrical constraints associated with the accommodation of environmental molecules at the interface. This oscillatory component allows for the existence of metastable equilibrium states. Experimental data on mica in water-containing atmospheres are then presented in support of this picture. In our experiments *hysteresis* is observed in cyclic loading tests: the work to *repropagate* the cracks through *healed* interfaces is found to be systematically lower than the original work to propagate the cracks through virgin material. Moreover, there are strong kinetic effects associated with the crack motion on displacement from equilibrium configurations. Simplistic linear elasticity calculations of the crack surface profiles indicate that, within the range of experimental crack extension forces, the interface is so constrained that the intrusive molecules must be limited in their motion by strong energy barriers. It is accordingly argued that the crack kinetics must be controlled by interface diffusion processes. Finally, a brief account of more sophisticated crack interface modelling of the full *non-linear* force functions now under way, with its attendant implications concerning the nature of the fracture chemistry, will be given.

It is acknowledged at the outset that some of the concepts developed here represent a radical departure from many of the traditional views of crack growth laws in highly brittle materials. The appeal of the surface force approach is that it provides a sound scientific basis for making, for the first time, *a priori* predictions of fracture behaviour. Conversely, it opens up the possibility of using controlled fracture testing as a useful adjunct to the surface force apparatus in the study of the physics and chemistry of confined interfaces.

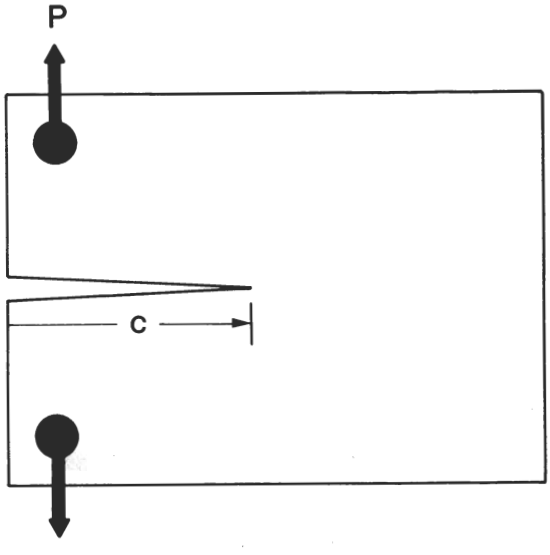

Fig. 1. Schematic of crack system.

2 FRACTURE MECHANICS AND SURFACE FORCE FUNCTIONS

2.1 Griffith-Irwin Fracture Mechanics

We begin with a statement of Griffith's theorem for equilibrium cracks [2, 3], expressed in Irwin's fracture mechanics notation [7, 8], to set the stage for incorporation of the surface force element. Consider a crack, characteristic dimension c, under remote load P, in a linear elastic solid, Fig. 1. The total energy of the system may be partitioned into mechanical and surface terms:

$$\begin{aligned} U &= U_M + U_S \\ &= U_M(P, c) + 2\gamma c \end{aligned} \tag{1}$$

For a virtual extension, dc, we may define a configurational force on the crack:

$$\begin{aligned} f &= -dU/dc = -dU_M/dc - dU_S/dc \\ &= G - 2\gamma \end{aligned} \tag{2}$$

The first term on the right is the Irwin crack *driving* force. The second term is the crack *resistance* term. (Note that we adopt a sign convention here such that both G and γ are defined as positive quantities.)

Equation 2 allows us to determine equilibrium states for the crack system. Specifically, the condition $f = 0$, $G = 2\gamma$, determines a state of *thermodynamic* equilibrium. For $G > 2\gamma$ the crack advances, for $G < 2\gamma$ it retracts (heals).

2.2 Surface Forces: Continuum Models

It is via the material–environment term γ in Equation 2 that the surface force notion enters the formulation. Consider the surface creation process in Fig. 2, whereby γ may be defined in terms of the work of separation

$$\gamma = \int_b^\infty p(y)\, dy \tag{3}$$

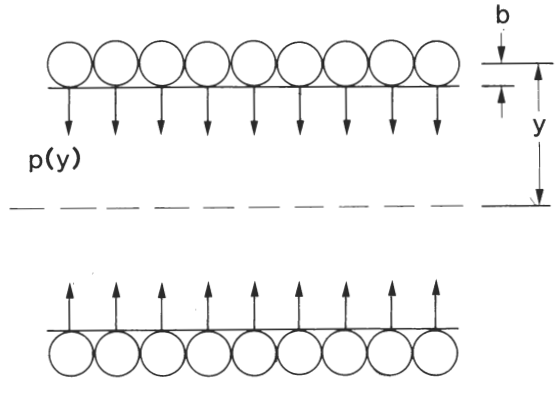

Fig. 2. Interfacial cohesion due to surface forces, p(y). Integral of these forces from equilibrium lattice half-spacing $y = b$ to $y = \infty$ defines the surface energy.

where b is the equilibrium lattice half-spacing of the material. (Note we take positive p to correspond to *attractive* cohesive forces, consistent with our sign convention for γ above.) Then p(y) is precisely the surface force function that researchers purport to measure directly on the Israelachvili-type apparatus. Hence γ may be independently predetermined, without any specific reference to a crack system.

The question now arises: how does environment influence γ? Consider first a strictly continuum model, where atomic structure of both solid material and fluid environment is ignored. In the context of brittle cracks this notion of continuum implies an unrestricted access of the environmental fluid to the near-tip bonds. We plot the general form of the appropriate potential energy vs. separation function for each of the two surfaces in Fig. 3, together with the corresponding force function $p(y) = dU(y)/dy$. Now suppose we take the system through the following cycle: (i) Begin with the surfaces in their original bound state ($U = -\gamma_0$); (ii) Separate the surfaces from $y = b$ to $y = \infty$, in vacuum ($U = 0$); (iii) Allow the environmental species to enter the system and adsorb onto the fully separated walls ($U = -\gamma_{AD}$); (iv) Allow the surfaces to recontact at $y = b$ ($U = -\gamma_{AD} - \gamma_1$). Then the appropriate surface energy for insertion in Equation 2 is

$$\gamma = \gamma_1 = \gamma_0 - \gamma_{AD} \qquad (4)$$

Hence the effect of environment on the crack energetics is simply to lower the surface energy from its vacuum value, γ_0, by the adsorption energy, γ_{AD}. This conclusion was first reached by Orowan [9]. In terms of the force function p(y) in Fig. 3, the effect

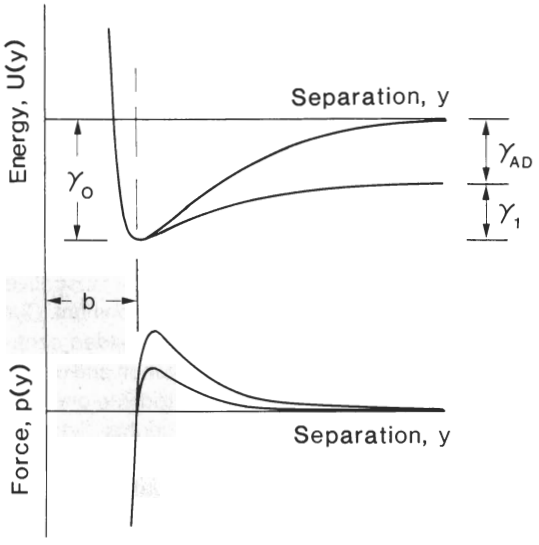

Fig. 3. Potential energy and corresponding surface force function for (half-) continuum *crack system in vacuum (upper curves) and fluid medium (lower curves). Effect of environment is to lower surface energy and thus to 'screen' wall–wall attractions.*

may be likened to a 'screening' of the primary surface interactions by the intervening medium.

There is, however, a major difficulty associated with this model. It is well documented that *non-equilibrium* cracks grow at some load-dependent *velocity*, e.g. as represented on a v–G plot. There is no inbuilt provision in our description thus far for explaining *kinetic* effects in brittle fracture; crack advance or retraction at $G \neq 2\gamma$ in a totally continuum system occurs spontaneously and reversibly. We must add a new element to the modelling. In keeping with the experience of the surface force researchers, we need to consider the essentially discrete structure of the solid–fluid–solid interface.

2.3 Surface Forces: Quasi-Discrete Models

We have indicated that the presence of a fluid at narrowly separated surfaces can give rise to oscillatory 'structural' forces [5]. Such oscillations reflect the radius of the solvent molecules. Evidently, the geometry of the molecules and the constraints associated with the packing give rise to a strong degree of ordering in the confined fluid. This unusual 'liquid' state must be expected to prevail at cohesive zones in brittle cracks, where the critical wall–wall separations are typically of atomic dimensions [10].

To illustrate this important role of geometrical constraint, let us consider how *water* molecules might penetrate a separating interface in *mica*. Mica, by virtue of its molecularly smooth cleavage, is our 'model' experimental material: it has been used almost exclusively in the surface force apparatus [4], and is ideally suited for crack reversibility studies [11]. Interplanar separation in the mica structure occurs across oxygen sheets which are 'glued' together by potassium ions, as shown in the elastic sphere model in Fig. 4 [1]. A little consideration reveals that the interstices in the undistorted layer structure in Fig. 4(a) are not large enough to accommodate intrusive water molecules; such an accommodation can only be effected if the oxygen sheets are normally strained by some 50%, as in Fig. 4(b). In terms of crack interfaces, this means that geometrical constraints must severely restrict the ingress of water and other reactive species to the critical tip region. These are precisely the conditions under which oscillatory structural forces [5] become manifest.

With this background, let us re-examine the potential energy and corresponding force functions, for a quasi-discrete surface–fluid–surface interface. We plot the appropriate functions in Fig. 5 [1]. The main distinction between these plots and their continuum counterparts in Fig. 3 is the presence of the subsidiary minima in U(y). Thus, curve 0 represents the intrinsic cohesion, and curves 1, 2, etc, represent the cohesion with corresponding integral numbers of molecule layers between the walls. Underlying the construction of these plots is the assumption that the intrusive

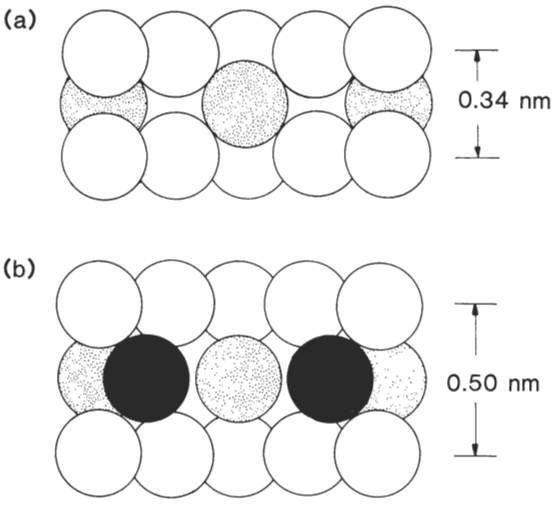

Fig. 4. Cleavage plane oxygen–potassium–oxygen layers in mica (profile view): (a) structure in equilibrium lattice; (b) same structure distorted to accommodate intrusive water molecules. Elastic sphere representations, O (open circles), K (shaded circles), H_2O (dark circles), using ionic radii.

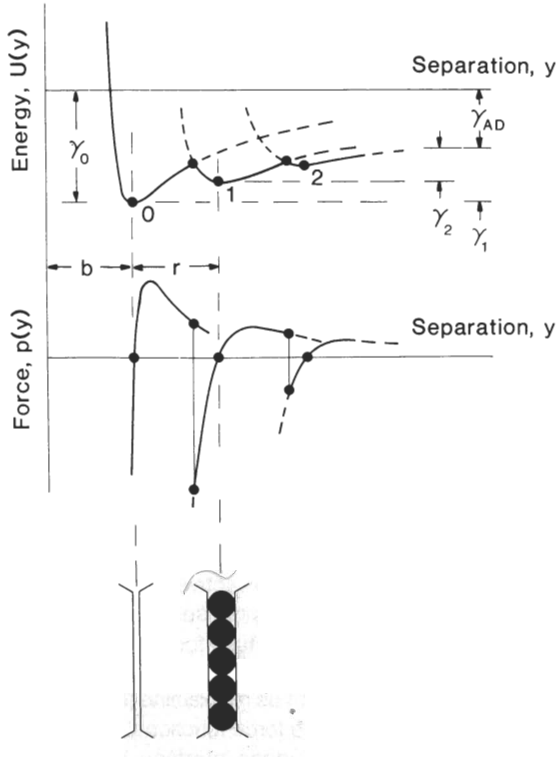

Fig. 5. Potential energy and corresponding surface force function for (half-) quasi-discrete crack system. Subsidiary minima in U(y), corresponding to integral numbers of molecule layers, allow for possibility of metastable equilibrium states.

molecules at any given separation are allowed to adjust their positions so as to minimize the system free energy. At large separations, the molecules are relatively free to make adjustments, in which case the interfacial fluid retains its bulk properties. However, as the interface narrows down, the molecules are forced by simple size restrictions to pack into an ordered structure, thereby accentuating the element of discreteness in the curves.

To see the implications of this element of discreteness, let us take the system through the same cycle as previously (Fig. 3). The first three stages may be effected as before: (i) Start with the surfaces in their intrinsically bound state at $y = b$ ($U = -\gamma_0$); (ii) Separate the surfaces along curve 0 to $y = \infty$, in vacuum ($U = 0$); (iii) Admit the adsorbant species to the fully separated walls ($U = -\gamma_{AD}$). It is with stage (iv), where we attempt to bring the surfaces together again, that differences arise. For there are now energy barriers to be overcome. If all the energy barriers can be overcome by thermal fluctuations then the intrinsic state at $y = b$ may indeed be restored ($U = -\gamma_{AD} - \gamma_1$); however, if the approach is too 'rapid', the system may become 'trapped' in one of the subsidiary minima at $y = b + nr$, r a molecular radius, along curves 1, 2, . . . ($U = -\gamma_{AD} - \gamma_2$). Then the appropriate surface energy for substitution into Equation 2 is either

$$\gamma = \gamma_1 = \gamma_0 - \gamma_{AD} \tag{5a}$$

(i.e. the same as Equation 4) at *thermodynamic* equilibrium, or

$$\gamma = \gamma_2, \quad (< \gamma_1) \tag{5b}$$

at *metastable* equilibrium.

There is compelling evidence, from mica–mica 'squeezing' experiments by Chan and Horn [12] in the surface force apparatus, to support the suggested existence of metastable equilibrium states. Those authors measured the expulsion rates of organic liquids down to near-contact, and noted discrete plateaus in the separation-time data. The distance between successive plateaus was of the order of one molecular diameter. The strong implications of those results concerning cyclic fracture behaviour, particularly in relation to the issues of kinetics and reversibility, will become evident in the following sections.

3 EXPERIMENTAL DATA ON MICA

We investigate the above principles with illustrative crack growth data on mica in a moist environment. Our system is a modification of the wedge-loaded cantilever beam configuration used by Obreimoff and others [11, 13–18]. Briefly, a wedge is inserted into one end of a mica flake and driven along the central cleavage plane by a stepper motor, Fig. 6. The crack extension force for any given length c is evaluated from the simple beam relation [8]

$$G = 3Eh^2d^3/4c^4 \tag{6}$$

where E is Young's modulus, h is the wedge half-thickness and d is the beam half-thickness. It is seen that G is a diminishing function of c, so the crack is

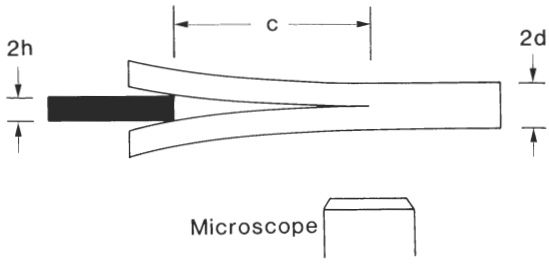

Fig. 6. Schematic of experimental arrangement for measuring cyclic crack behaviour in mica.

mechanically stable. Thus we can make the crack advance or retract in a controlled manner, simply by reversing the wedge-drive motor. The crack response is monitored visually by mounting the entire assembly onto the stage of an inverted microscope.

Most of the previous work cited in References 11 and 13–17 above has focused on stationary crack configurations, by allowing a 'decent period of time' to elapse after each adjustment of the wedge position. In this way it is assumed that the system has reached a true equilibrium state, so that G in Equation 2 may be properly identifiable with an appropriate γ term. In our experiments we have also investigated the *time-dependent approach* to any such equilibrium state; specifically, we have measured forward–backward–forward velocities for wedge load–unload–reload (L–U–R) cycles over a wide range of G. From these measurements we can plot a sequence of v–G curves, encapsulating all the kinetic *and* equilibrium features of our material–environment system onto a single master diagram.

Figure 7 is such a data plot for mica in moist (55% RH) laboratory air. The dashed line at right, which summarizes the results of a few control runs in dry nitrogen gas, may be taken as representative of an *inert* environment. The velocity is plotted in the usual logarithmic co-ordinates (negative values in the lower portion of the diagram corresponding to crack retraction). The features of interest in the curves for the air environment are as follows: (i) The G values required to drive the crack at any given rate are substantially lower than for the nitrogen environment, attesting to the deleterious influence of water; (ii) The slopes are steep in the region of velocity reversal at $G \approx 400–500$ mJ.m^{-2}, indicative of a strong threshold behaviour; (iii) The curve for *reloading* relative to that for the initial *loading* appears to be shifted to a lower point along the G axis, suggesting a certain hysteresis in the crack reversibility; (iv) The curves at the extremes of the G range tend to 'plateaus', at velocities around $\pm 10^{-3}$m.s.$^{-1}$.

These results pose us with interesting new questions in connection with kinetics and reversibility: how do we reconcile the hysteretic velocity thresholds with the equilibrium γ quantities defined in Section 2?; what

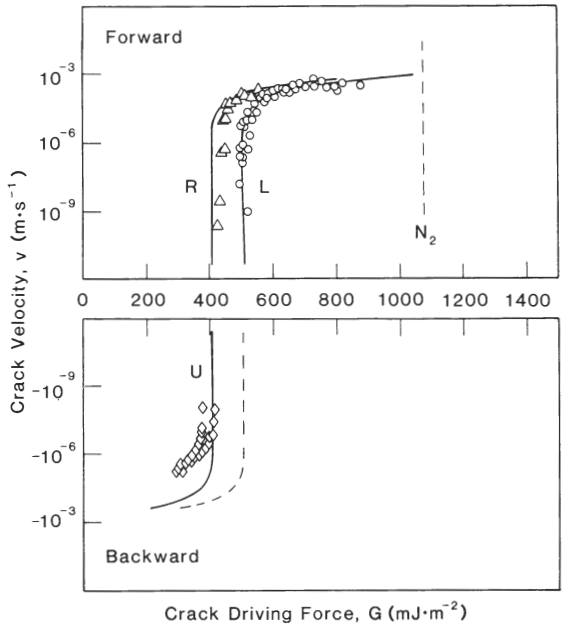

Fig. 7. Crack velocity vs. crack driving force for mica in air (55% RH). Data are for initial crack advance in virgin material on initial loading (L), crack retraction on wedge unloading (U), crack advance through healed interface on reloading (R). Solid curves are fits to theoretical function, Equation 9.

is the underlying mechanism of kinetic growth in non-equilibrium states? To gain important clues to these questions we need to look closely at the actual crack profiles in the near-tip regions where the critical interaction processes are expected to operate.

4 CRACK PROFILES AND CRACK KINETICS

4.1 Irwin Linear Elastic Solutions of the Crack Profile

We have taken pains to emphasize the essential elements of discreteness and non-linearity in the cohesive force function that underlies the surface energy terms in the Griffith fracture theorem. A proper description of the crack profile clearly must take these elements into account. Having acknowledged this necessity, let us nevertheless make our first evaluation of the crack profile using the continuum linear elastic displacement solutions of Irwin [7, 8]. The reader may recall that these solutions are based on the hypothesis that the crack tip is concentrated at a point; ahead of the tip the cohesive bonds remain intact (Hooke's law satisfied everywhere), behind the tip they are completely severed (traction-free walls). We shall see that even the Irwin approximation is sufficient to provide insight into the kinetic and hysteretic behaviour, provided we recognize the lattice structure in the analysis, i.e. we use the solutions to locate *atom centres* rather than walls of infinitesimally narrow slits, Fig. 8. The subtleties of more complex non-linear analyses we defer to Section 5.

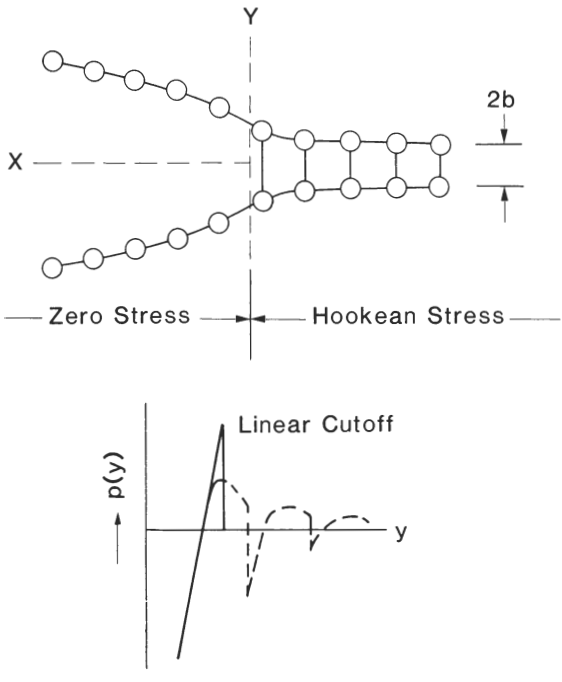

Fig. 8. 'Irwin profile' of brittle crack, calculated using linear elastic solutions for displacement fields at atom centres along lattice rows immediately adjacent to cleavage plane. Lower diagram indicates linear portion of total p(y) function 'sampled' in the Irwin approximation.

Accordingly, we compute the normal displacements of the atom centres in the (oxygen) cleavage-plane layers at $y = \pm b$ in the mica structure [1] using the displacement function [7, 8]

$$u(x, b) = (K/E)(x/2\pi)^{1/2} f(x/b) \qquad (7)$$

where $K = (GE)^{1/2}$ is the stress intensity factor. The results of such computations are shown in Fig. 9 for four values of G, embracing the data range of the v–G plot in Fig. 7. In these profiles the potassium ions are taken to attach alternately to upper and lower surfaces, consistent with the requirements of charge neutrality. The water molecules are allowed to occupy interfacial interstitial sites to the point where the walls narrow down below the maximum-penetration configuration of Fig. 4(b).

It is immediately clear that, contrary to most traditional thinking, the environmental species do not necessarily have unrestricted access to the crack tip. (Recall that the tip in the Irwin formulation is *well defined*, at 0–0 in Fig. 9.) Indeed, noting that the data range in Fig. 7 lies somewhere between configurations b and c in Fig. 9, we conclude that the intrusive molecules will experience much lattice constriction in their passage along the interface. This suggests the existence of diffusional energy barriers, thus providing the basis for an explanation of the kinetic behaviour.

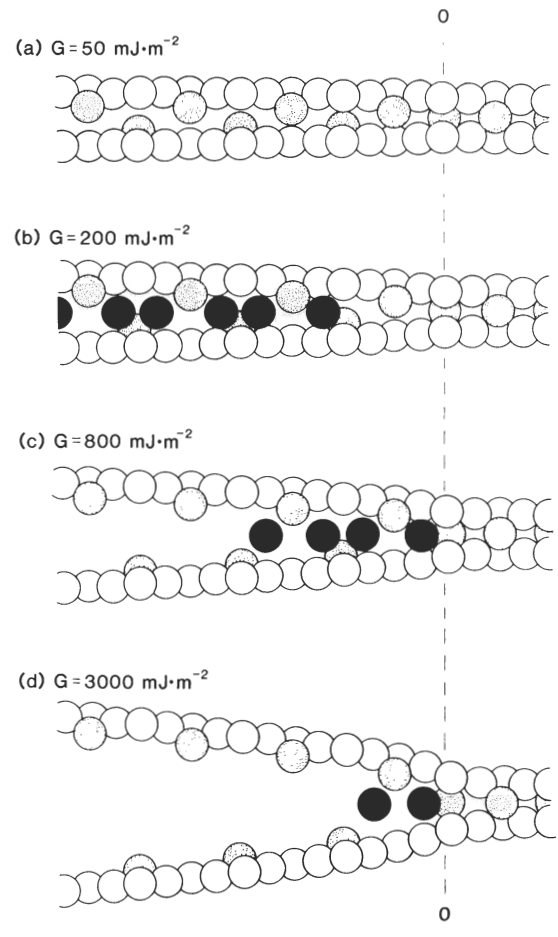

Fig. 9. Irwin crack profiles in mica, for four G values. Cleavage occurs between O layers (open circles), linked by K ions (shaded circles). Water molecules (dark circles) are allowed to penetrate interface to point of equilibrium accommodation, Fig. 4(b).

4.2 Stress-Enhanced Interface Diffusion and the v–G Function

We can now construct a thermal activation model, albeit phenomenological, to explain the v–G behaviour. We envisage a process of rate-limiting interfacial diffusion over energy barriers, as in Fig. 10. (Of course, these barriers will become 'tighter' as the interface narrows: strictly, our argument here applies most effectively to the *leading* molecules.) The activation process may occur in either the forward or backward direction, depending on the relative heights of the barriers U_+ and U_- in Fig. 10. From Maxwell-Boltzmann statistics we may write immediately:

$$v = v_0\{\exp(-U_+/kT) - \exp(-U_-/kT)\} \qquad (8)$$

where v_0 is a characteristic velocity for the material–environment system. The stress dependence enters via the biasing effect of the applied loading on the barrier heights. It can be demonstrated [19] for any

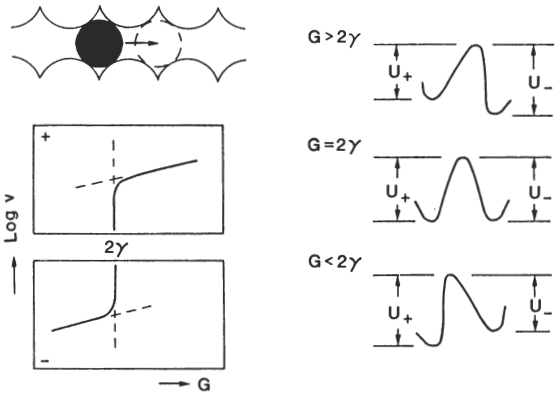

Fig. 10. Model for interfacial diffusion of molecules into crack cohesive zone. Energy barriers to the diffusion are biased by the applied loading on the crack, as quantified by G.

thermally activated process that this dependence is linear in G for small departures from the Griffith equilibrium configuration, so Equation 8 may be rewritten

$$v = v_o \sinh[(G-2\gamma)/2\Gamma] \qquad (9)$$

where Γ is another characteristic material–environment parameter. Note that this equation is totally consistent with the Griffith energy balance theorem: at $G = 2\gamma$, $v = 0$ (thermodynamic equilibrium); at $G > 2\gamma$, $v > 0$ (rate-dependent crack advance—forward fluctuations dominant); at $G < 2\gamma$, $v < 0$ (rate-dependent crack healing—reverse fluctuations dominant).

We include a schematic plot of Equation 9 in Fig. 10. It will be noted that the sinh function contains provision to account for the steep slope of the v–G curves close to the equilibrium point and the strong plateau behaviour away from this point. However, this still leaves one major element of the curves unaccounted for, the hysteresis; we must take the description one stage further.

4.3 Metastable States and Hysteresis

To explain the hysteresis in the v–G behaviour in load–unload–reload cycles we need only recall our earlier assertion in Section 2.3 of a molecular-scale discreteness in the underlying surface force function (Fig. 5). There we alluded to the possibility of the environmentally exposed crack interface becoming 'trapped' in metastable states. In terms of surface energy, this trapping corresponds to a reduction from γ_1 to γ_2 in Equation 5.

Figure 11 depicts the hysteretic mechanism envisaged in the loading–unloading–reloading cycle. At upper left we sketch the idealised adsorption–desorption process that would have to operate if the velocity were to be completely reversible. This reversible process is represented by the sinh curve with quiescent point $G = 2\gamma_1$ in the schematic v–G plot in Fig. 11. In practice, however, we would expect

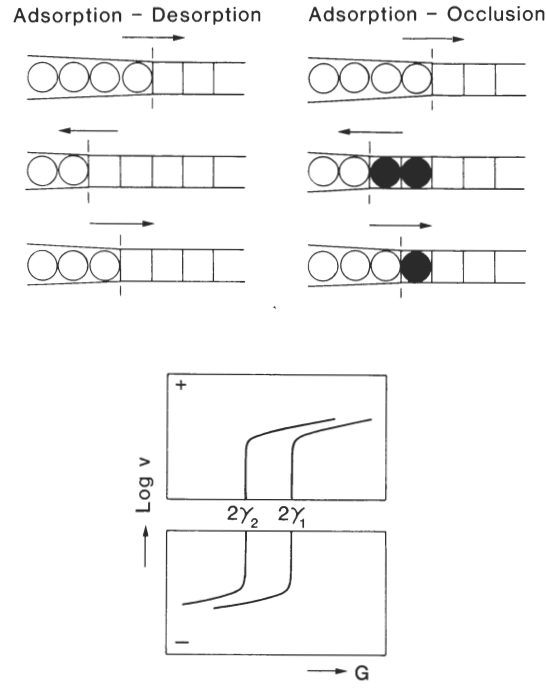

Fig. 11. Schematic of environmentally influenced crack behaviour in load–unload–reload cycle. (a) Adsorption-desorption model, in which penetrating molecules are completely expelled during crack closure (complete healing and reversibility). (b) Adsorption-occlusion model, where molecules are trapped in metastable states (dark circles) on closure (incomplete healing and reversibility). (c) Schematic v–G plots corresponding to the processes depicted in (a) and (b).

total desorption to occur under only the most extraordinary circumstances; e.g. infinitely slow reversal of the applied loading, to allow for expulsion of the confined molecules over the energy barriers. The drainage experiments of Chan and Horn [12] referred to earlier attest to the difficulty in achieving such expulsion. The adsorption–occlusion process sketched at upper right in Fig. 11 is therefore more likely to be representative of the real crack behaviour. The 'contamination' of the interface in this latter case simply means that the lower portion of the above v–G curve is effectively bypassed; on unloading (and reloading) the crack the quiescent point shifts to $G = 2\gamma_2$ (i.e. equivalent to translating the entire sinh curve laterally to the left on the v–G diagram).

The curves through the data in Fig. 7 were fitted in accordance with this interpretation. Specifically, these curves were obtained by fixing v_o and Γ in Equation 9 and separately adjusting γ_1 and γ_2 to match the respective L and U–R data.

5 NON-LINEAR SOLUTIONS: THE 'MOLECULAR WEDGE'

It is important to acknowledge that the treatment in the previous section, while useful in providing

phenomenological models of the v–G behaviour, contains an important internal contradiction. We made an emphatic statement in Section 2 that surface forces are critical in determining interfacial properties. These forces are *essentially non-linear*, yet in Section 4 we adopted the Irwin linear solutions for crack displacement fields. We concluded from the resulting profiles in Fig. 8 that the crack walls are so narrow as to exert strong constraint on the intrusive molecules. If this is so then there must be significant interaction (via these intrusive molecules) between the walls behind the Irwin tip; i.e. the oscillatory 'tail' of the p(y) function must certainly be active. The analysis in Section 4 is not self-consistent.

To obtain self-consistency, we need to modify Equation 7 to allow for the additional effect of the non-linear portion of the p(y) function [20, 21]. Consider the crack system in Fig. 12. In this diagram the cohesive zone is separated into primary and secondary zones. The boundary between the two is delineated by the point of maximum penetration of the intrusive molecules (Fig. 5). The distribution of surface forces along the crack plane, p(x), has to be determined from p(y) (included at right in Fig. 12), which means we need to know, *a priori*, the functional dependence y(x). In other words, in order to obtain the solution for the crack profile we have to know this solution beforehand.

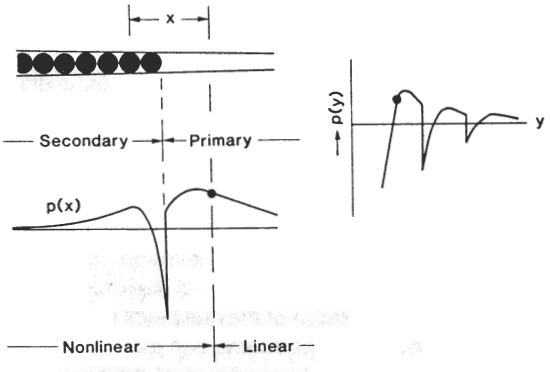

Fig. 12. Distribution of non-linear surface forces across crack plane. Function p(x) sketched here as laterally inverted form of p(y) (taking x and y to be linearly related for simplicity).

This apparent impasse is given mathematical expression [21] by appropriately adding a second, non-linear term (incorporating non-linear components of the primary as well as the secondary forces) to the displacement relation in Equation 7:

$$u(x,b) = (K/E)(x/2\pi)^{1/2} f(x/b) + \int_0^{\infty} g(x/b, x')\, p(x')\, dx' \qquad (10)$$

where x is a field point and x′ a source point for the surface forces, and g(x/b, x′) is a Greens function. Equation 10 is a non-linear integral equation for which, in the absence of any prior knowledge of p(x′), there are no closed-form solutions.

Thus to proceed further one is forced to resort to numerical analysis, by computer modelling. Such numerical modelling has been started in these laboratories by R. M. Thomson [22]. It is not our intent to elaborate on the details of this modelling here, other than to emphasize the need to match the surface force function p(y) to critical parameters of the fracture system, e.g. surface energies (γ_0, γ_1, γ_2), lattice half-spacing (b), and molecular radius (r) (Fig. 5). Rather, we restrict ourselves to brief mention of a broader insight into the wall–molecule–wall interaction process emerging from these preliminary computations. In particular, we focus on the interesting conclusion by Thomson [22] that the interaction may be viewed in terms of a 'molecular wedge'.

To establish a proper perspective for discussing the molecular wedge concept it is useful to recall the Griffith equilibrium relation in Section 2: from Equations 2 (f = 0) and 4 we have

$$G = 2\gamma_0 - 2\gamma_{AD} \qquad (11)$$

This relation is pertinent to an 'external' (or 'macroscopic') observer. Such an observer, located outside the crack interface, perceives (via the mechanically applied loading) the effect of the molecular adsorption quantity $2\gamma_{AD}$ as a true lowering of the surface energy on the right hand side of the Griffith equation (i.e. in accord with the Orowan hypothesis [9]. Suppose, however, we rearrange Equation 11:

$$G + 2\gamma_{AD} = 2\gamma_0 \qquad (12)$$

We thus obtain an equivalent form of the Griffith equation, appropriate to an 'internal' ('microscopic') observer. This observer, located within the primary cohesive zone (Fig. 12), regards the crack tip as an inviolate configuration, characterized by the vacuum surface energy $2\gamma_0$; the quantity $2\gamma_{AD}$ in this case is interpreted as a ('fictitious') mechanical driving force which augments G on the left side of Equation 12. It is in this latter context of a superimposed configurational force that the molecular wedge is conceived.

With this background, we sketch in Fig. 13 the crack structure suggested by Thomson's preliminary computations. The geometrical feature that distinguishes this structure from that in the Irwin profiles (Fig. 9) is the elastic conformation of the solid walls to the intruding molecules. Thomson pictures the molecules as being 'sucked' into the ever-narrowing crack interface by the attractive component of the secondary surface force function (to the immediate right of subsidiary minimum 1 in Fig. 5) until, in the highly constrained near-tip region, the repulsive, electron-cloud overlap component (immediate left of minimum 1) asserts itself. The latter component, because of its closer proximity to the tip, exerts a dominant influence on the net driving force; hence the 'wedge'.

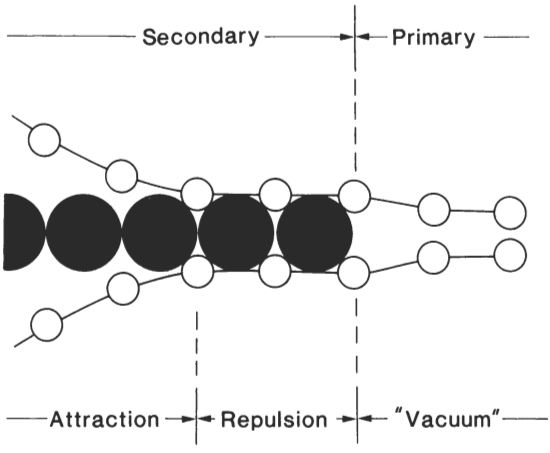

Fig. 13. Schematic of Thomson molecular wedge concept, showing various cohesive zones.

It should be emphasized here that this interpretation of the role of the $2\gamma_{AD}$ term in the Griffith balance is somewhat tentative. Final confirmation awaits more detailed computations than are yet available. Some searching questions need to be asked. For instance, Thomson's analysis focuses almost exclusively on the most penetrative of the environmental molecules. Is it not possible that the repulsive forces that contribute to the wedge effect are of a much longer range than this? After all, the (oscillatory) structural forces measured in the surface force apparatus extend over *several* molecular dimensions [5]. Or, alternatively, is it possible that the principal action of the molecules in relation to the primary cohesion is not so much that of a superposed mechanical wedge as of a partial electrostatic screen [23] (e.g. as alluded to earlier in Section 2.2, but with the screening forces now confined to the secondary zone)? More questions than answers, perhaps, but a sign that there is much fundamental information to be gained from surface force modelling of brittle fracture systems.

6 FINAL IMPLICATIONS

We have presented a view of chemically enhanced fracture in which the critical growth conditions are determined uniquely by fundamental surface forces. We believe this view to hold for all ceramics and other truly brittle materials, for which the crack tips are atomically sharp [24]. As a corollary, we assert that the crack-tip configurations for a given material–environment system will have a certain quality of invariance [25]. These contentions have a certain aesthetic appeal to those who would seek to present fracture theory as a well-founded scientific discipline. In this context it is well not to forget that we are dealing with a subject hitherto plagued by a multitude of empirical 'laws' and a seemingly endless number of hypothetical crack-tip structures.

With these general comments, let us examine two important specific problem areas in brittle fracture in which the surface force idea has a strong impact:

(i) *Thresholds.* Zero-velocity thresholds on v–G plots, of the kind seen in the steeply sloped regions in Fig. 7, occur *naturally* as equilibrium solutions of the quasi-discrete modelling outlined in Section 2.3 [1, 25–27]. Moreover, this modelling, by virtue of its provision for metastable states, accounts for the threshold hysteresis in load–unload–reload cycles. Previously, the threshold phenomenon was cited as indisputable evidence for the breakdown of the atomically-sharp-crack concept (e.g. by 'rounding' of the tip contour by chemical dissolution or plastic flow) [25].

(ii) *Crack velocity mechanisms.* The profile solutions discussed in Sections 4 and 5 indicate that the fracture kinetics in mica (Fig. 7) are largely governed by interfacial diffusion of molecular species. This is a radical conclusion. The overwhelmingly accepted view of "slow crack growth" in brittle solids is that of the 'concerted reaction' [28], where the interaction with environmental species is pictured as completely localized at a single line of crack-tip bonds. Our modelling suggests that the concerted reaction may occur under only exceptional circumstances, e.g. in 'open-structured' silicate glasses at higher G levels such that the reactive molecules can penetrate without restriction to the (Irwin) tip. In materials like mica [1] and sapphire [1, 29] (and, we believe, most other ceramics) the relatively dense lattice structures ensure the existence of strong interfacial barriers to such penetration, in which case the notion of an extended secondary interaction zone behind the tip (Fig. 12) is more appropriate.

As a final remark, let us note that just as surface forces may be used to shed light on brittle fracture behaviour, so may the reverse be true. Thus far, experiments with the surface force apparatus have been restricted to one material, mica. No such restriction is apparent in the fracture testing of brittle materials. If solutions to the crack interface problem posed in Section 5 can be obtained we have the prospect that fracture mechanics, so long the exclusive province of the mechanical engineer, might find use as a supplementary tool in the study of surface chemistry at the molecular level.

ACKNOWLEDGEMENTS

The authors wish to thank D. H. Roach, R. M. Thomson, R. F. Cook, and R. G. Horn for many stimulating discussions on various aspects of this study, and L. Descotes for analysis of the data in Fig. 7. This work was supported by the U.S. Office of Naval Research, Ceramics and Metallurgy Program.

REFERENCES

1. B. R. Lawn, D. H. Roach and R. M. Thomson, *J. Mater. Sci.*

2. A. A. Griffith, *Philos. Trans. Roy. Soc. Lond.*, 1920, **A 221**, 163.
3. B. R. Lawn and T R. Wilshaw, *Fracture of Brittle Solids*, Cambridge University Press, London, 1975, Ch. 1.
4. J. N. Israelachvili, *Intermolecular and Surface Forces*, Academic Press, London, 1985.
5. R. G. Horn and J. N. Israelachvili, *J. Chem. Phys.*, 1981, **75**, 1400.
6. H. K. Christenson, R. G. Horn and J. N. Israelachvili, *J. Colloid Interface Sci.*, 1982, **88**, 79.
7. G. R. Irwin, in *Handbuch der Physik*, Springer-Verlag, Berlin, 1956, Vol. 6, p. 551.
8. B. R. Lawn and T. R. Wilshaw, *Fracture of Brittle Solids*, Cambridge University Press, London, 1975, Ch. 3.
9. E. Orowan, *Nature*, 1944, **154**, 341.
10. B. R. Lawn and T. R. Wilshaw, *Fracture of Brittle Solids*, Cambridge University Press, London, 1975, Ch. 4.
11. A. I. Bailey and S. M. Kay, *Proc. Roy. Soc. Lond*, 1967, **A 301**, 47.
12. D. Y. C. Chan and R. G. Horn, *J. Chem. Phys.*, 1985, **85**, 5311.
13. J. W. Obreimoff, *Proc. Roy. Soc. Lond.*, 1930, **A 127**, 47.
14. B. V Derjaguin and M. S. Metsik, *Sov. Phys.—Solid State*, 1960, **1**, 1393.
15. A. I. Bailey, *J. Appl. Phys.*, 1961, **32**, 1407.
16. P. J. Bryant, L. H. Taylor and P. L. Gutshall, in *Trans. Tenth Nat. Vacuum Sympos.*, Macmillan, New York, 1983, p. 21.
17. G. Trott, P. L. Gutshall and J. M. Phillips, in *Proc. Seventh Internat. Vac. Congress and Third Internat. Conf. Solid Surfs.*, Vienna, 1977, p. 1051.
18. D. H. Roach, D. M. Heuckeroth and B. R. Lawn, *J. Colloid and Interface Sci.*, 1986, **114**, 292.
19. B. R. Lawn and T. R. Wilshaw, *Fracture of Brittle Solids*, Cambridge University Press, London, 1975, Ch. 8.
20. G. I. Barenblatt, *Adv. Appl. Mechs.*, 1962, **7**, 55.
21. R. A. Schapery, *Int. J. Fracture*, 1975, **11**, 141.
22. R. M. Thomson, in preparation.
23. G. L. Gaines and D. Tabor, *Nature*, 1956, **178**, 1304.
24. B. R. Lawn, B. J. Hockey and S. M. Wiederhorn, *J. Mater. Sci.*, 1980, **15**, 1207.
25. B. R. Lawn, K. Jakus and A. C. Gonzalez, *J. Am. Ceram. Soc.*, 1985, **68**, 25.
26. B. R. Lawn, *Appl. Phys. Letters*, 1985, **47**, 809.
27. D. R. Clarke, B. R. Lawn and D. H. Roach, in *Fracture Mechanics of Ceramics* (eds. R. C. Bradt, A. G. Evans, D. P. H. Hasselman and F. F. Lange), Plenum, New York, 1986, Vol. 8, p, 341.
28. T. A. Michalske and S. W. Freiman, *Nature*, 1982, **295**, 511.
29. R. F. Cook, *J. Mater. Res.*, 1986, **1**, 852.